

Supplementary Information

Crystal Structures and Local Environments of NASICON-type Na₃FeV(PO₄)₃ and Na₄FeV(PO₄)₃ Positive Electrode Materials for Na- ion Batteries

Sunkyu Park^{1,2,3}, Jean-Noël Chotard^{1,5}, Dany Carlier^{2,5}, Iona Moog³, Matthieu Courty¹,
Mathieu Duttine², François Fauth⁴, Antonella Iadecola⁵, Laurence Croguennec^{2,5} and
Christian Masquelier^{1,5}

¹ *Laboratoire de Réactivité et de Chimie des Solides, Université de Picardie Jules Verne,
CNRS-UMR 7314, F-80039 Amiens Cedex 1, France*

² *CNRS, Univ. Bordeaux, Bordeaux INP, ICMCB UMR 5026, F-33600 Pessac, France*

³ *TIAMAT, 15 Rue Baudelocque, 80000 Amiens*

⁴ *CELLS-ALBA Synchrotron, Cerdanyola del Vallès, E-08290 Barcelona, Spain*

⁵ *RS2E, Réseau Français sur le Stockage Electrochimique de l'Energie, FR CNRS 3459,
F-80039 Amiens Cedex 1, France*

Table S1. Room temperature ^{57}Fe Mössbauer refined parameters, isomer shift (δ), quadrupole splitting (Δ), Full-Width at Half-Maximum (Γ) and Relative Area (%), of the target composition $\text{Na}_4\text{FeV}(\text{PO}_4)_3$ obtained through various synthesis conditions.

Synthesis conditions	Sites	δ (mm/s)	Δ (mm/s)	Γ (mm/s)	Rel. Area (%)
Solid-state in Ar	Fe ^{III}	0.46(2)	0.36(2)	0.43(2)	11(3)
	Fe ^{II} (1)	1.26(1)	2.15(1)	0.35(1)	70(3)
	Fe ^{II} (2)	1.21(2)	2.36(2)	0.25(2)	11(3)
	Fe ^{II} (3)	1.12(1)	1.50(2)	0.27(2)	8(3)
Sol-gel in Ar/H ₂	Fe ^{III}	0.47(2)	0.36(2)	0.41(2)	9(3)
	Fe ^{II} (1)	1.25(1)	2.13(2)	0.36(2)	78(3)
	Fe ^{II} (2)	1.20(2)	2.35(2)	0.28(2)	10(3)
	Fe ^{II} (3)	1.10(2)	1.47(3)	0.27(2)	3(3)
Sol-gel in Ar	Fe ^{III}	0.50(2)	0.40(2)	0.44(2)	31(3)
	Fe ^{II} (1)	1.22(1)	2.07(1)	0.40(1)	64(3)
	Fe ^{II} (2)	1.19(2)	2.34(2)	0.28(2)	5(3)
NaFePO ₄ [ref. 1]	Fe ^{II} (2)	1.2	2.19	—	
Na ₃ Fe ₂ (PO ₄) ₃ [ref. 2]	Fe ^{III}	0.451(3)	0.326(6)	0.282(5)	

The Fe^{II}(3) site tends to appear with more sodiated phase. Although tiny peaks around $Q = 1 \text{ \AA}^{-1}$ from the XRD patterns (see inset of FigureS1-3) were observed with more sodiated phase, further investigation is required to determine the origin of the signal.

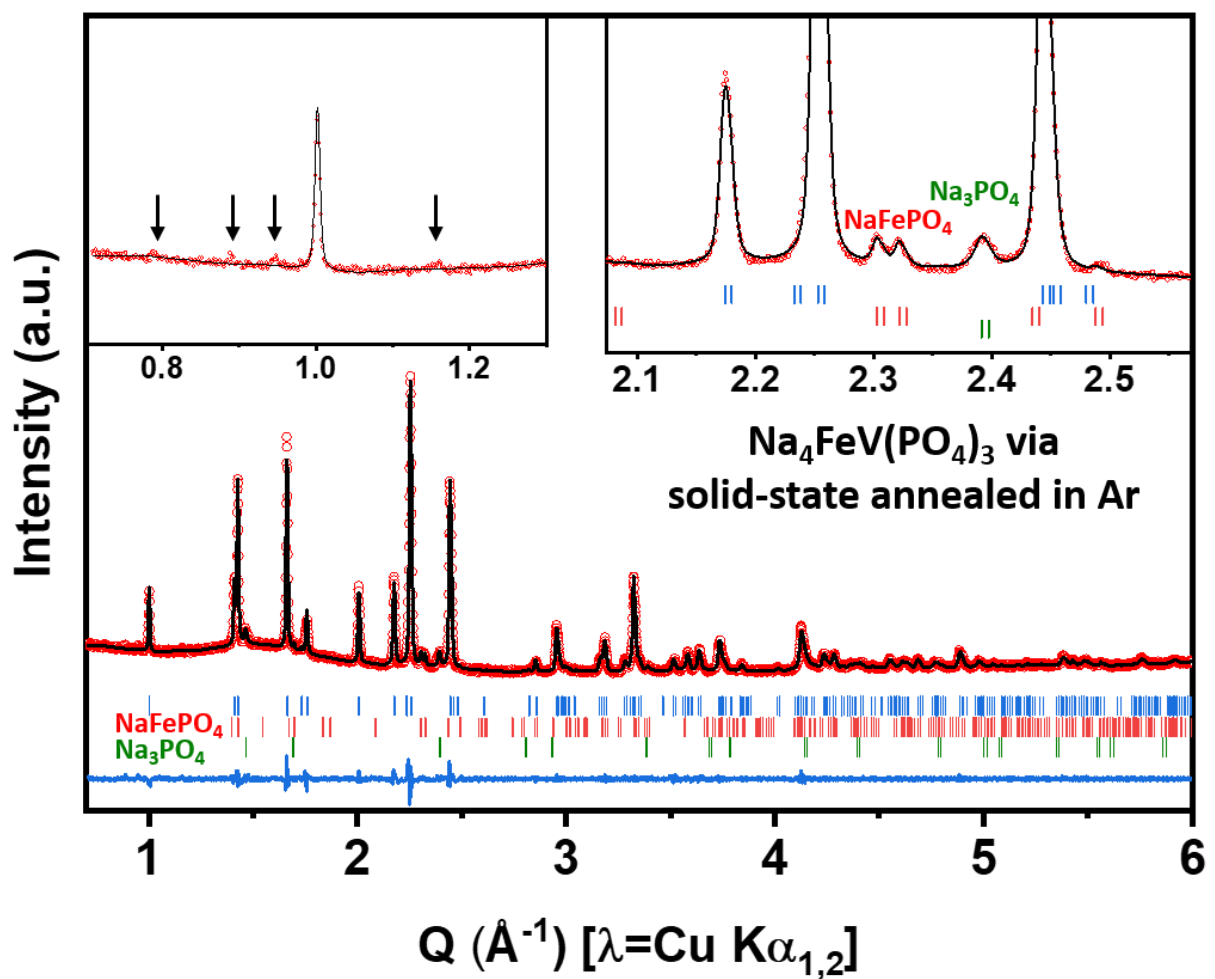


Figure S1. Le Bail fitting of the target composition $\text{Na}_4\text{FeV}(\text{PO}_4)_3$ obtained through solid-state synthesis in Ar.

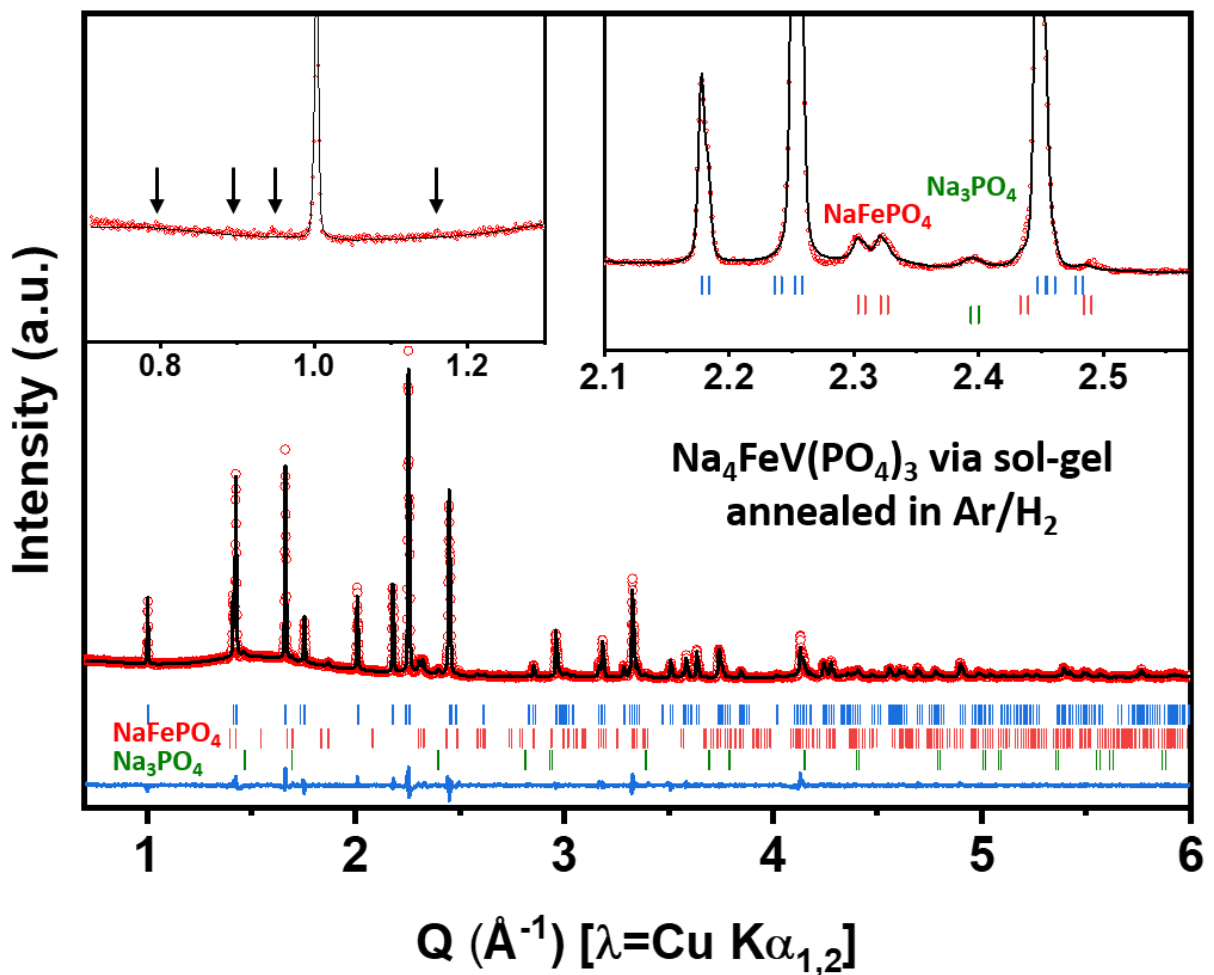


Figure S2. Le Bail fitting of the target composition $\text{Na}_4\text{FeV}(\text{PO}_4)_3$ obtained through sol-gel synthesis followed by an annealing in Ar/H_2

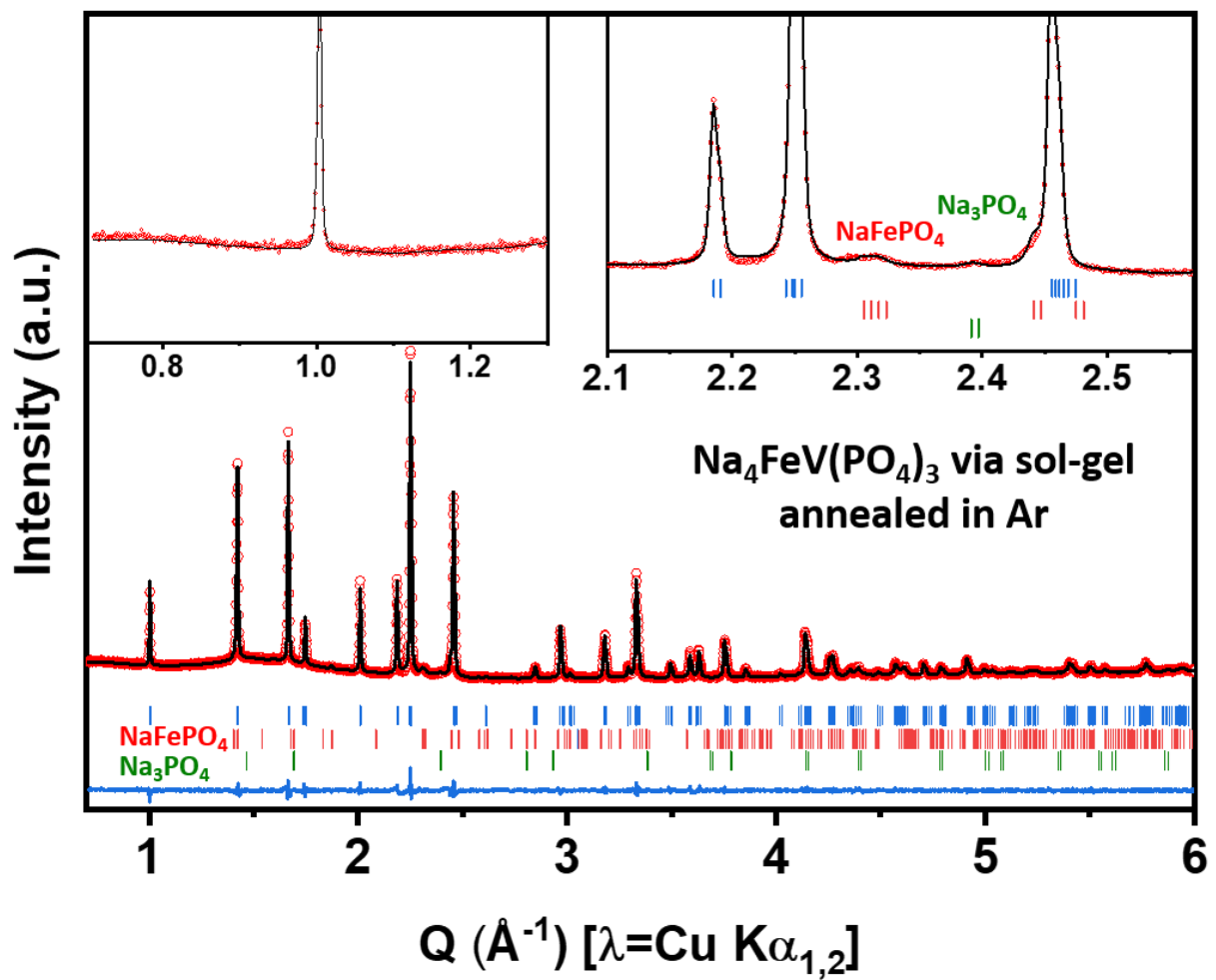


Figure S3. Le Bail fitting of the target composition $\text{Na}_4\text{FeV}(\text{PO}_4)_3$ obtained through sol-gel synthesis followed by an annealing in Ar

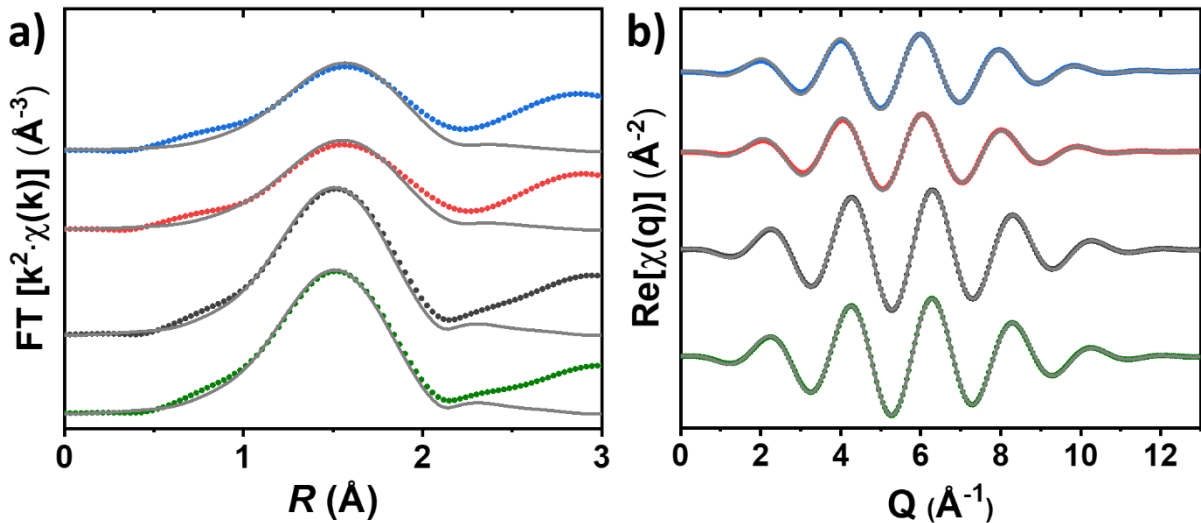


Figure S4. **a)** k^2 -weighted Fourier transforms of Fe K-edge EXAFS oscillations collected for $\text{Na}_3\text{Fe}_2(\text{PO}_4)_3$ (green), $\text{Na}_3\text{FeV}(\text{PO}_4)_3$ (black), and for the electrochemically sodiated samples obtained at cut-off voltages of 2 V (red) and 1.3 V (blue). **b)** Corresponding backward Fourier transforms in q -space.

Table S2. Refined parameters of first shell of Fe K-edge EXAFS spectra. k -range: 2.6 - 10.8 \AA^{-1} , R-range: 1.0 - 2.1 \AA , $dR = 0$, sine window.

Sample	$d(\text{Fe} - \text{O}) (\text{\AA})$	$E_o (\text{eV})$	$\sigma^2 (\text{\AA}^2)$	R-factor
$\text{Na}_4\text{FeV}(\text{PO}_4)_3$ / cut-off at 1.3 V	2.067(5)	0.1	0.0121(5)	0.009
$\text{Na}_{3+x}\text{FeV}(\text{PO}_4)_3$ / cut-off at 2.0 V	2.053(5)	0.2	0.0122(5)	0.012
$\text{Na}_3\text{FeV}(\text{PO}_4)_3$ / as-synthesized	1.986(5)	0.4	0.0071(5)	0.002
$\text{Na}_3\text{Fe}_2(\text{PO}_4)_3$ / reference	1.986(5)	0.3	0.0074(5)	0.001

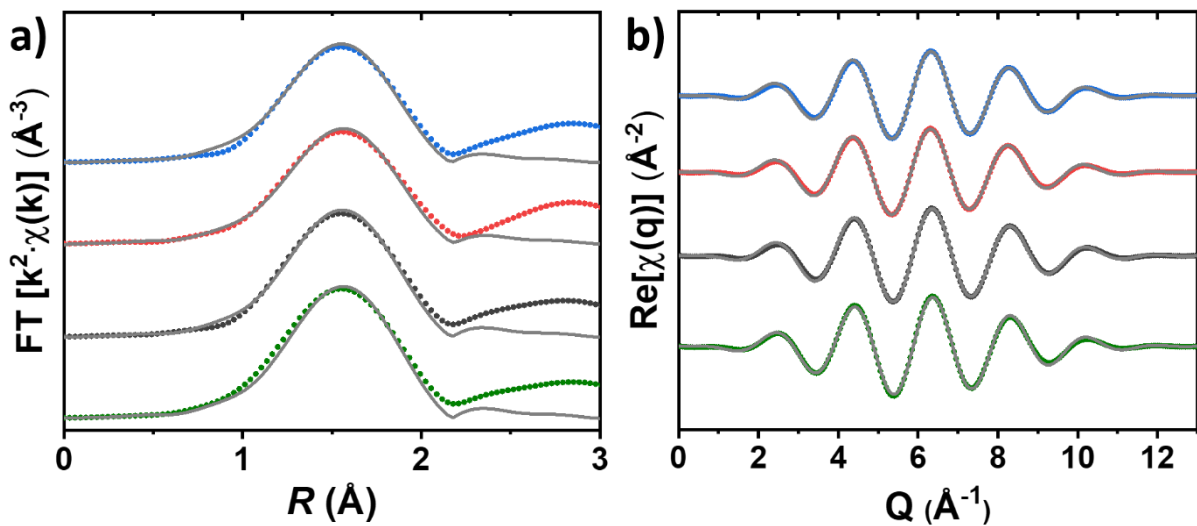


Figure S5. **a)** k^2 -weighted Fourier transforms of V K-edge EXAFS oscillations collected for $\text{Na}_3\text{V}_2(\text{PO}_4)_3$ (green), $\text{Na}_3\text{FeV}(\text{PO}_4)_3$ (black), and for the samples electrochemically sodiated at cut-off voltages of 2 V (red) and 1.3 V (blue). **b)** Corresponding backward Fourier transforms in q -space.

Table S3. Refined parameters of first shell of V K-edge EXAFS spectra. k -range: $2.7 - 10.7 \text{\AA}^{-1}$, R -range: $1.0 - 2.2 \text{\AA}$, $dR = 0$, sine window.

Sample	$d(\text{V} - \text{O}) (\text{\AA})$	$E_\text{o} (\text{eV})$	$\sigma^2 (\text{\AA}^2)$	R-factor
$\text{Na}_4\text{FeV}(\text{PO}_4)_3$ / cut-off at 1.3 V	2.023(5)	-1.1	0.0038(5)	0.0091
$\text{Na}_{3+x}\text{FeV}(\text{PO}_4)_3$ / cut-off at 2.0 V	2.033(5)	0.2	0.0041(5)	0.0078
$\text{Na}_3\text{FeV}(\text{PO}_4)_3$ / as-synthesized	2.018(5)	0.1	0.0032(5)	0.0107
$\text{Na}_3\text{V}_2(\text{PO}_4)_3$ / reference	2.018(5)	1.1	0.0028(5)	0.0095

Table S4. Room temperature ^{57}Fe Mössbauer refined parameters of $\text{Na}_3\text{FeV}(\text{PO}_4)_3$ and electrochemically sodiated samples at cut-off voltages of 2 V and 1.3 V.

Sample	Sites	δ (mm/s)	Δ (mm/s)	Γ (mm/s)	Rel. Area (%)
$\text{Na}_4\text{FeV}(\text{PO}_4)_3$ cut-off 1.3 V (Sample C)	Fe^{III}	0.47(2)	0.50(2)	0.38(2)	13(3)
	Fe^{II}	1.24(1)	2.25(2)	0.38(1)	87(3)
$\text{Na}_{3+x}\text{FeV}(\text{PO}_4)_3$ cut-off 2.0 V (Sample B)	Fe^{III}	0.47(2)	0.46(3)	0.34(2)	26(2)
	Fe^{II}	1.23(1)	2.23(1)	0.37(2)	74(2)
$\text{Na}_3\text{FeV}(\text{PO}_4)_3$ as-synthesized (Sample A)	Fe^{III}	0.46(1)	0.33(1)	0.28(1)	97(3)
	Fe^{II}	1.15(2)	2.10(4)	0.34(3)	3(3)
$\text{Na}_3\text{Fe}_2(\text{PO}_4)_3$ [ref. 2]	Fe^{III}	0.451(3)	0.326(6)	0.282(5)	

The overall oxidation states of ex-situ samples obtained by Mössbauer spectroscopy may slightly differ from those obtained by X-ray absorption spectroscopy as it was difficult to measure the two different techniques with the same samples.

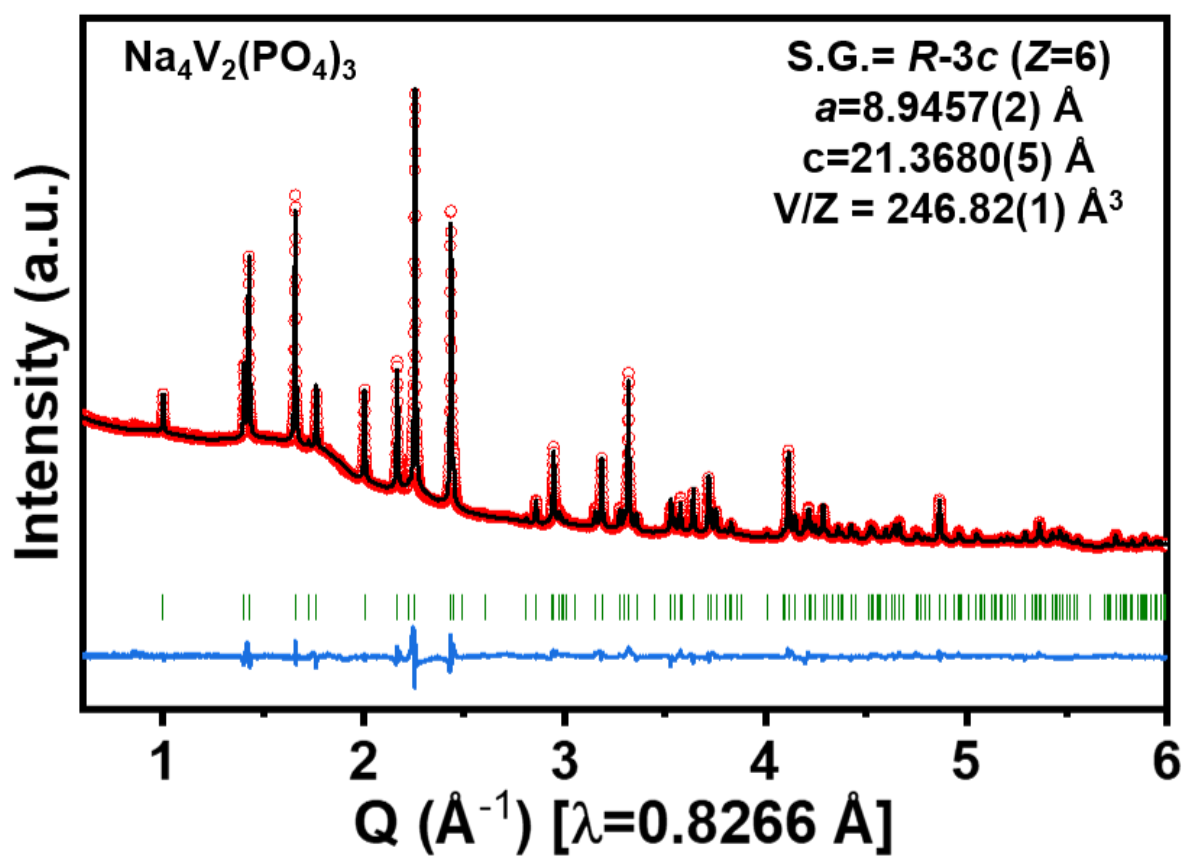


Figure S6. Rietveld refinement of Na₄V₂(PO₄)₃ obtained from Na₃V₂(PO₄)₃ through electrochemical sodiation.

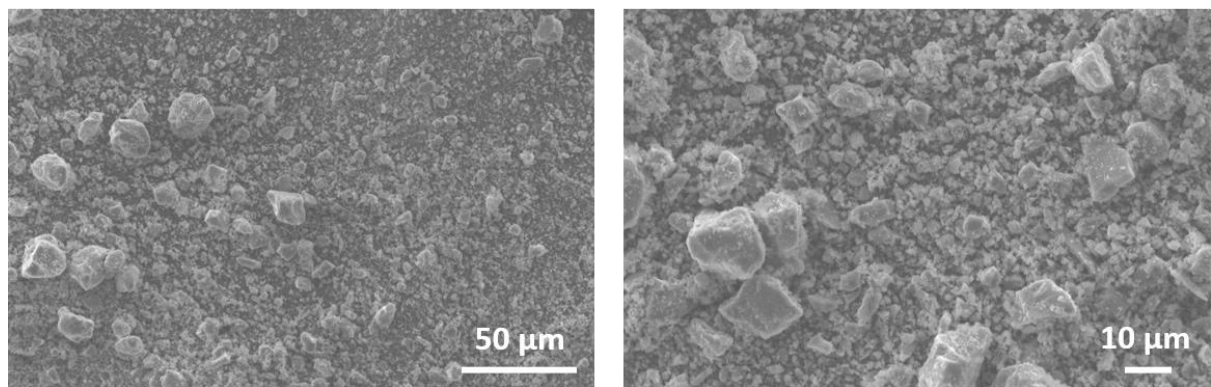


Figure S7. SEM images of as-synthesized $\text{Na}_3\text{FeV}(\text{PO}_4)_3$

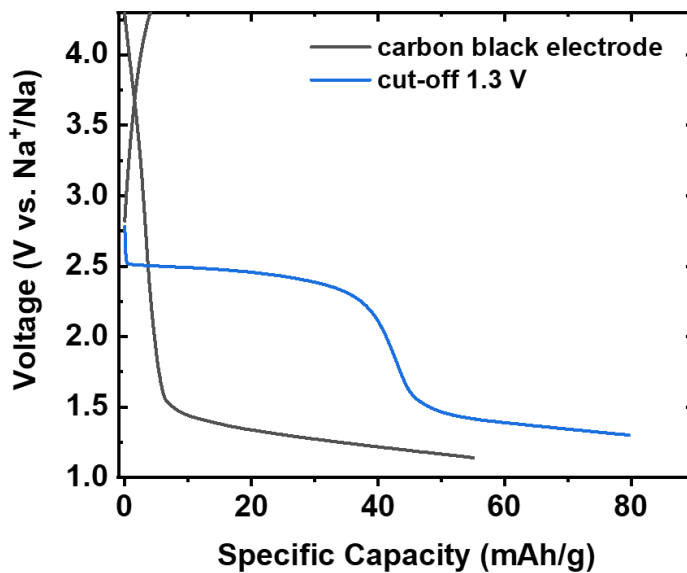


Figure S8. Comparison of the electrochemical curves of carbon black electrode and $\text{Na}_3\text{FeV}(\text{PO}_4)_3$ electrode with a cut-off voltage of 1.3 V vs. Na^+/Na (sample C).

References

- (1) Kosova, N. V.; Podugolnikov, V. R.; Devyatkina, E. T.; Slobodyuk, A. B. Structure and Electrochemistry of NaFePO_4 and $\text{Na}_2\text{FePO}_4\text{F}$ Cathode Materials Prepared via Mechanochemical Route. *Mater. Res. Bull.* **2014**, *60*, 849–857. <https://doi.org/10.1016/j.materresbull.2014.09.081>.
- (2) Idczak, R.; Tran, V. H.; Świątek-Tran, B.; Walczak, K.; Zajac, W.; Molenda, J. The Effects of Mn Substitution on the Structural and Magnetic Properties of the NASICON-Type $\text{Na}_3\text{Fe}_{2-x}\text{Mn}_x(\text{PO}_4)_3$ Solid Solution. *J. Magn. Magn. Mater.* **2019**, *491*, 1–11. <https://doi.org/10.1016/j.jmmm.2019.165602>.